JGR Biogeosciences

RESEARCH ARTICLE
10.1029/2024JG008233

Eroding Permafrost Coastlines Release Biodegradable Dissolved Organic Carbon to the Arctic Ocean

Emily M. Bristol[1,2], Megan I. Behnke[3,4], Robert G. M. Spencer[3], Amy McKenna[3,5], Benjamin M. Jones[6], Diana L. Bull[7], and James W. McClelland[1,8]

[1]Department of Marine Science, The University of Texas at Austin, Port Aransas, TX, USA, [2]Now at U.S. Geological Survey, Pacific Coastal & Marine Science Center, Santa Cruz, CA, USA, [3]Department of Earth, Ocean, and Atmospheric Science, Florida State University, Tallahassee, FL, USA, [4]Now at Alaska Coastal Rainforest Center, University of Alaska Southeast, Juneau, AK, USA, [5]Department of Soil and Crop Sciences, Colorodo State University, Fort Collins, CO, USA, [6]Institute of Northern Engineering, University of Alaska Fairbanks, Fairbanks, AK, USA, [7]Climate Systems, Sandia National Laboratories, Albuquerque, NM, USA, [8]The Ecosystems Center, Marine Biological Laboratory, Woods Hole, MA, USA

Abstract Coastal erosion mobilizes large quantities of organic matter (OM) to the Arctic Ocean where it may fuel greenhouse gas emissions and marine production. While the biodegradability of permafrost-derived dissolved organic carbon (DOC) has been extensively studied in inland soils and freshwaters, few studies have examined dissolved OM (DOM) leached from eroding coastal permafrost in seawater. To address this knowledge gap, we sampled three horizons from bluff exposures near Drew Point, Alaska: seasonally thawed active layer soils, permafrost containing Holocene terrestrial and/or lacustrine OM, and permafrost containing late-Pleistocene marine-derived OM. Samples were leached in seawater to compare DOC yields, DOM composition (chromophoric DOM, Fourier transform ion cyclotron resonance mass spectrometry), and biodegradable DOC (BDOC). Holocene terrestrial permafrost leached the most DOC compared to active layer soils and Pleistocene marine permafrost. However, DOC from Pleistocene marine permafrost was the most biodegradable (33 ± 6% over 90 days), followed by DOC from active layer soils (23 ± 5%) and Holocene terrestrial permafrost (14 ± 3%). Permafrost leachates contained relatively more aliphatic and peptide-like formulae, whereas active layer leachates contained relatively more aromatic formulae. BDOC was positively correlated with nitrogen-containing and aliphatic formulae, and negatively correlated with polyphenolic and condensed aromatic formulae. Using estimates of eroding OM, we scale our results to estimate DOC and BDOC inputs to the Alaska Beaufort Sea. While DOC inputs from coastal erosion are relatively small compared to rivers, our results suggest that erosion may be an important source of BDOC to the Beaufort Sea when river inputs are low.

Plain Language Summary Arctic coastlines are rapidly eroding into the ocean. Soils along these coastlines contain large quantities of organic matter (OM) that dissolves in seawater and may be consumed by microbes. If this dissolved organic matter (DOM) is biodegradable, it can be an important energy source to coastal food webs and/or quickly decomposed to greenhouse gases. We used laboratory experiments to examine the chemical composition of the DOM that is released from eroding soils into seawater and measured its biodegradability. We compared results for three different layers of soil at Drew Point, Alaska, including near-surface soils that thaw seasonally and deeper soils that are perennially frozen (permafrost). Our results show that different layers, which contain OM of different sources and ages, have distinct chemical characteristics that impact biodegradability. While rivers supply more OM to the Alaska Beaufort Sea than coastal erosion, our results show that DOM released from all soil layers is highly biodegradable, and that DOM from deep permafrost is the most biodegradable. We deomonstrate that coastal erosion can be an important source of OM to Arctic coastal ecosystems, particularly in locations and seasons (e.g., late summer) that receive fewer river inputs.

Key Points:

- Eroding soils and permafrost along the Alaska Beaufort Sea coast leach biodegradable dissolved organic carbon into seawater
- Biodegradability was higher in leachates from Late-Pleistocene relict marine permafrost than Holocene terrestrial soils and permafrost
- Permafrost leached aliphatic and peptide-like molecular formulae that were not present or less abundant in active layer soils

Supporting Information:

Supporting Information may be found in the online version of this article.

Correspondence to:

E. M. Bristol,
bristol@utexas.edu

Citation:

Bristol, E. M., Behnke, M. I., Spencer, R. G. M., McKenna, A., Jones, B. M., Bull, D. L., & McClelland, J. W. (2024). Eroding permafrost coastlines release biodegradable dissolved organic carbon to the Arctic Ocean. *Journal of Geophysical Research: Biogeosciences*, *129*, e2024JG008233. https://doi.org/10.1029/2024JG008233

Received 6 MAY 2024
Accepted 18 JUL 2024

Author Contributions:

Conceptualization: Emily M. Bristol, Diana L. Bull, James W. McClelland
Data curation: Emily M. Bristol, Megan I. Behnke
Formal analysis: Emily M. Bristol, Megan I. Behnke, Robert G. M. Spencer, James W. McClelland
Funding acquisition: Diana L. Bull, James W. McClelland
Investigation: Emily M. Bristol, Amy McKenna, Benjamin M. Jones
Methodology: Emily M. Bristol, Robert G. M. Spencer, Amy McKenna, James W. McClelland
Software: Emily M. Bristol

1. Introduction

The Arctic Ocean is strongly influenced by terrestrial inputs of organic matter (OM) and other nutrients, impacting biogeochemical cycling and estuarine ecosystem dynamics (McClelland et al., 2012). Large rivers have been well studied across the Arctic, and are known to contribute massive quantities of OM to the Arctic Ocean,

Supervision: Benjamin M. Jones, Diana L. Bull, James W. McClelland
Visualization: Emily M. Bristol, Megan I. Behnke
Writing – original draft: Emily M. Bristol
Writing – review & editing: Emily M. Bristol, Megan I. Behnke, Robert G. M. Spencer, Amy McKenna, Benjamin M. Jones, Diana L. Bull, James W. McClelland

largely in the dissolved form (Holmes et al., 2012; McClelland et al., 2016). Dissolved organic carbon (DOC) from permafrost watersheds tends to be relatively biodegradable, with a notable proportion rapidly utilized by microbes (Vonk et al., 2015). In the estuarine environment, this terrestrial OM acts as an energy subsidy for nearshore heterotrophs and accumulates in marine food webs (Bell et al., 2016; Dunton et al., 2012). Remineralization of terrestrial OM also releases inorganic nutrients that support a substantial amount of marine primary production in the Arctic Ocean (Tank et al., 2012; Terhaar et al., 2021).

Rapidly eroding Arctic coastlines also release terrestrial OM to the ocean, yet very few studies have examined the composition or biodegradability of eroded organic carbon (OC). Erosion currently mobilizes an estimated 8.5–15.4 Tg OC yr^{-1} to the Arctic Ocean (Nielsen et al., 2022; Terhaar et al., 2021). While this erosional OC flux is less than OC flux from rivers draining the pan-Arctic watershed (34 Tg DOC yr^{-1}, Holmes et al., 2012; 5.8 Tg particulate OC yr^{-1}, McClelland et al., 2016), eroding coastlines may be an important source of biolabile OC at certain places or times of the year. Riverine DOC fluxes and biodegradability peak in June during the spring freshet (Behnke et al., 2021; Drake et al., 2018; Spencer et al., 2015; Textor et al., 2019; Vonk et al., 2015; Wologo et al., 2021), whereas erosion peaks later, occurring during the summer open water season when waves and storms are more active (Irrgang et al., 2022). Furthermore, coastal erosion rates and associated OC fluxes are forecasted to increase by a factor of ∼1.5 by 2100 due to Arctic warming and sea ice decline (Nielsen et al., 2022). While research on the fate of eroding permafrost in the marine environment is limited, initial studies that incubated bulk soils and permafrost in seawater show that eroding OC can be rapidly decomposed in the marine environment (Tanski et al., 2019, 2021).

While erosion primarily mobilizes OC in the particulate form, this material may be leached to dissolved forms (Dou et al., 2008) that are readily utilized by microbial communities (Bruhn et al., 2021). Here, we examine the composition and biodegradability of DOC that is rapidly released from eroding bluffs in seawater. To simulate DOC release in the coastal ocean, we leached active layer soils and permafrost from Drew Point, Alaska in Beaufort Sea surface water. Leachates were incubated over 26 and 90 days in dark, aerobic conditions to measure DOC loss due to microbial uptake or remineralization (i.e., biodegradable DOC; BDOC). Additionally, we used chromophoric dissolved organic matter (CDOM) measurements and ultra-high resolution Fourier-transform ion cyclotron resonance mass spectrometry (FT-ICR MS) to examine the composition of leached dissolved organic matter (DOM). While these methods have been used to assess the composition and biolability of DOC in freshwaters across the Arctic (Behnke et al., 2021; Drake et al., 2018; Spencer et al., 2015; Textor et al., 2019; Vonk et al., 2015; Wologo et al., 2021), this is the first study to link BDOC with high-resolution DOM compositional data from permafrost leached in seawater. Finally, we scale these results to assess the biogeochemical and ecological importance of BDOC leached from eroding material along the Alaska Beaufort Sea coast.

2. Study Area

The Alaska Beaufort Sea coast is fringed by barrier islands and shallow estuarine waters that, despite being ice covered for approximately 9 months of the year, are highly productive. These shallow lagoons and coastal waters are vital habitat for anadromous and marine fish (Stanek et al., 2022), migratory waterfowl (Richardson & Johnson, 1981), bowhead whales (Schell et al., 1989), and other marine mammals that are important for local Iñupiat subsistence fishing and hunting. The Alaska Beaufort Sea receives freshwater, OM, and nutrients from rivers draining the North Slope of Alaska during the spring freshet in June and throughout the summer open water season until freeze up in early October (McClelland et al., 2014). In addition, much of the coastline is eroding, retreating at an average rate of 1.9 m yr^{-1}, and at maximum annual rates of 25 m yr^{-1} (Figure 1; Gibbs & Richmond, 2017). This coastal permafrost erosion supplies large quantities of OM to the nearshore Beaufort Sea (Bristol et al., 2021; Ping et al., 2011).

This study focuses on Drew Point, a section of exposed coastline located ∼100 km southeast of Utqiaġvik. Similar to much of the North Slope of Alaska, the terrain near Drew Point consists mainly of thermokarst lakes and drained lake basins (B. M. Jones & Arp, 2015; B. M. Jones et al., 2022). Underneath tundra soils and reworked lake sediments, deeper permafrost at Drew Point contains relict marine sediment deposited during a late-Pleistocene marine transgression (Figure 2; Bristol et al., 2021; Dinter et al., 1990). Bluffs are tall (1.6–7.1 m) compared to most of the Alaska Beaufort Sea coast, and therefore store large stocks of OC above sea level (∼86 kg OC m^{-2} for an average 3.7 m bluff; Bristol et al., 2021; Ping et al., 2011). Moreover, erosion rates at

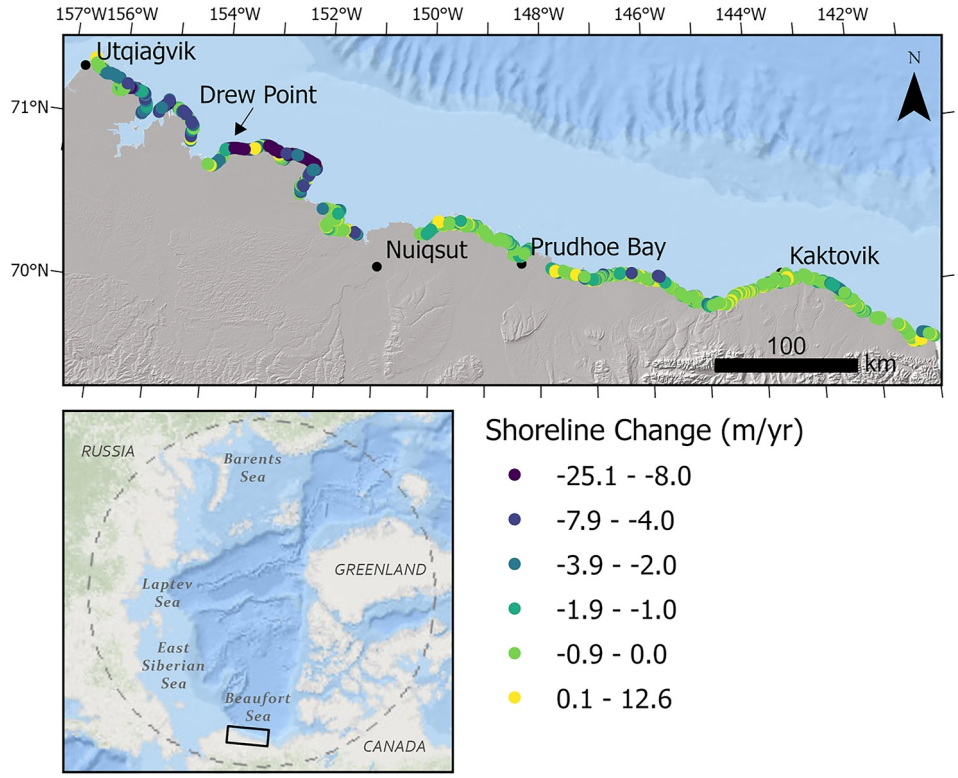

Figure 1. Short term (1980s–2010s) average shoreline change rates for protected and exposed mainland coastline along the Alaska Beaufort Sea (Gibbs & Richmond, 2017). Negative values indicate shoreline loss. The Arctic Ocean basemap was compiled by ESRI.

Drew Point are extremely rapid and increasing over time, currently averaging ~17.2 m yr^{-1} (Figure 1; Jones et al., 2018). Recent OC fluxes from just a 9 km stretch of coastline near Drew Point (12,332 Mg OC yr^{-1}) are similar to OC fluxes from the Kuparuk River, which is the third largest river draining the North Slope of Alaska (Bristol et al., 2021; McClelland et al., 2014).

Figure 2. (a) Example of an eroding bluff near Drew Point, Alaska. "Active layer" refers to the seasonally thawed terrestrial soils near the tundra surface. "Holocene terrestrial permafrost" refers to perennially frozen Holocene-age terrestrial soils and/or lacustrine sediments. "Pleistocene marine permafrost" refers to relict marine sediment that was deposited during a Late-Pleistocene marine transgression, but that is presently located above and below sea level in eroding bluffs.
(b) Collecting permafrost samples by coring horizontally into an exposed bluff at the young drained lake basin site near Drew Point, Alaska.

3. Methods

3.1. Sample Collection

Active layer and permafrost samples were collected from exposed bluffs near Drew Point during August 2019 (Figure 2). Three active layer samples, three shallow permafrost samples, and three deeper permafrost samples were collected from a young (500 years BP) drained thermokarst lake basin (Hinkel et al., 2003; M. C. Jones et al., 2012). An additional three active layer samples were sampled from primary material that has never been reworked by thaw-lake cycles. Samples from the drained lake basin were collected by scraping thawed material from an exposed bluff face before coring horizontally with a 7.5 cm diameter SIPRE core auger. Due to tall (~6 m), steep bluffs at the primary surface site, active layer samples were collected by drilling vertically from the tundra surface to a depth of approximately 35 cm; these cores were subsampled to capture a similar depth range as horizontal cores. The SIPRE core barrel was wiped clean in between samples, and the average depth of the sample was measured from the tundra surface. Core sections were stored in clean Ziplock bags inside coolers packed with ice or frozen permafrost and transported back to the Barrow Arctic Research Center in Utqiagvik, Alaska by helicopter or float plane. Samples were stored in a freezer at −20°C at the Barrow Arctic Research Center until transported frozen back to the University of Texas Marine Science Institute. Seawater used for the experiment was collected from Beaufort Sea surface waters offshore from Kaktovik, AK during August 2018, filtered through pre-combusted Whatman GF/F (0.7 μm) filters, transported frozen to the University of Texas Marine Science Institute, and stored at −20°C. The seawater had a salinity of 31.

3.2. Dissolved Organic Carbon Leaching

Active layer and permafrost samples were thawed at 4°C and gently homogenized. Then, subsamples were taken to measure total organic carbon (TOC) content. After subsampling, the homogenized soil/sediments were refrozen, so that TOC could be quantified before leaching. Slurries were formed by combining thawed soil/sediment samples with 700 mL GF/F filtered seawater in pre-combusted beakers. We normalized the soil/sediment TOC added to each slurry with a target concentration of 5 g TOC L^{-1}. This was equivalent to ~75–550 g wet soil/sediment L^{-1}, depending on TOC and water content. This TOC to seawater ratio was chosen so that leachate DOC concentrations would be roughly similar to each other, and so that DOC concentrations would high enough to quantify low percent DOC losses (i.e., BDOC) precisely. Leachate DOC ranged from 4.6 to 38 mg DOC L^{-1} (see associated data set for more detail; Bristol et al., 2024). These values are within range of DOC concentrations measured in shallow coastal waters, rivers, and/or supra-permafrost groundwater in the region (Beaufort Lagoon Ecosystem LTER, 2024; Bristol, 2023; Connolly et al., 2020). To act as a control, one beaker contained only Beaufort Sea surface water. The slurries and seawater control were covered, stored in the dark, and gently stirred three times throughout the leaching period. After 24 hr, the slurries and seawater control were decanted and vacuum filtered using pre-combusted GF/F filters.

3.3. Biodegradable Dissolved Organic Carbon

To facilitate comparison with other studies, we generally followed the standardized biodegradable dissolved organic carbon (BDOC) protocol suggested by Vonk et al. (2015). This lability assay measures DOC loss throughout an incubation, often 28 days at room temperature, in the dark to prevent photochemical reactions or primary production. Initial samples were 0.7 μm filtered before the incubation, removing particulate matter but allowing some microbial biomass to pass through. At the end of the incubation period, samples were re-filtered (0.7 μm) to remove any bacterial aggregates that may have formed. Therefore, the DOC loss represents DOC that was respired and/or incorporated into microbial biomass.

Immediately after filtering the slurries, each leachate and the seawater control were subsampled for initial chemical analyses (i.e., DOC concentration, CDOM, FT-ICR MS). Acid washed, pre-leached polycarbonate bottles were used throughout the experiment. Each leachate and the seawater control were incubated in triplicate in the dark on a shaker table in an environmental chamber and sampled at 26 and 90 days. The incubation temperature averaged 19°C. Bottles were sealed to prevent evaporation but had a 1:1 solution to headspace ratio and were uncapped for 10 minutes weekly while on the shaker table to allow fresh air into the headspace and underlying water. After 26 and 90 days, triplicate sets of bottles were re-filtered using pre-combused GF/F filters and subsampled for DOC and CDOM analyses.

3.4. Bulk Geochemical Analyses

Subsamples for soil/sediment TOC (%) analysis were acidified with 10% ultrapure HCl in silver capsules before carbon mass was analyzed with a Thermo Fisher EA-Isolink-CNSOH elemental analyzer. Concentrations of DOC were measured with a Shimadzu TOC-V CSH analyzer. Samples were acidified to a pH of 2 with concentrated HCl (ACS reagent grade; JT Baker) immediately after filtering and DOC concentrations were analyzed within 24 hr. BDOC was measured as the percent loss of leached DOC (i.e., leachate DOC concentration minus seawater control DOC concentration) between the initial and final timepoints of the incubation. The Beaufort Sea surface water sample contained 1.2 mg DOC L^{-1}, and there was no detectible change in seawater DOC concentrations throughout the incubation experiment. There was no correlation between DOC concentrations and BDOC measurements, indicating that initial leachate DOC concentrations did not impact decomposition rates.

Subsamples for CDOM were stored at 4°C and measured within 24 hr using an Ocean Optics UV-visible light absorbance spectrophotometer. Ultrapure water blanks were run approximately every five samples, and sample spectra were blank corrected. Parameters $S_{275–295}$ (log-transformed spectral slope between 275 and 295 nm) and S_R (275–295 nm slope:350–400 nm slope) were calculated from CDOM spectra according to Helms et al. (2008). The specific ultra-violet absorbance at 254 nm ($SUVA_{254}$; decadic absorbance at 254 nm normalized by DOC concentration) was calculated according to Weishaar et al. (2003). All bulk chemical analyses were completed at the University of Texas Marine Science Institute.

3.5. Fourier Transform Ion Cyclotron Resonance Mass Spectrometry

Leachate DOM samples for 21 T FT-ICR MS analyses were solid phase extracted onto reverse phase BondElut PPL cartridges (100 mg; Agilent) following an established protocol (Dittmar et al., 2008). Briefly, leachate subsamples were acidified to a pH of 2 with HCl, passed through pre-conditioned PPL cartridges, rinsed with acidified water, and eluted with 1 mL methanol for a target concentration of 40 μg C mL^{-1}. ACS reagent grade HCl (JT Baker) and LC/MS grade methanol and water (Fisher Chemical) were used throughout.

Extracts were stored in methanol at −20°C until analysis on a custom-built hybrid linear ion trap 21 T FT-ICR MS at the National High Magnetic Field Laboratory in Tallahassee, Florida (Hendrickson et al., 2015; Smith et al., 2018) with negative electrospray ionization. For each spectrum, 100 time domain acquisitions were conditionally co-added. Mass spectra were phase-corrected (Xian et al., 2010) and elemental compositions iteratively assigned to peaks with signal magnitude >6σ root-mean-square baseline noise (Bahureksa et al., 2022; O'Donnell et al., 2016) with PetroOrg © TM software (Corilo, 2015). Formulae were assigned using elemental constraints of $C_{1–45}H_{1–92}O_{0–35}N_{0–4}S_{0-2}$ and with a mass accuracy ≤300 ppb (Table S1 in Supporting Information S1). The modified aromaticity index (AI_{mod}) was calculated from the neutral elemental composition to provide qualitative measure of the degree of aromaticity (Koch & Dittmar, 2006, 2016). Elemental ratios and AI_{mod} were used to correlate elemental compositions to compound classes defined by atomic elemental ratios of H/C and O/C: polyphenolics ($0.5 < AI_{mod} \leq 0.66$); condensed aromatics ($AI_{mod} > 0.66$); highly unsaturated and phenolics ($AI_{mod} \leq 0.5$, $H/C < 1.5$, $O/C \leq 0.9$); aliphatic ($1.5 \leq H/C \leq 2.0$, $O/C \leq 0.9$, and $N = 0$); sugar-like ($O/C > 0.9$); and peptide-like ($1.5 \leq H/C \leq 2.0$, and $N > 0$) (Behnke et al., 2021). Each assigned molecular formula may contain multiple isomers, and compound structure cannot be assessed from direct infusion mass spectrometry of DOM with any mass detector. The relative abundance of each formula was calculated by normalizing each peak magnitude to the sum of all peak magnitudes assigned in each sample. The relative abundance (expressed as percentages; %RA) of each compound class and elemental composition grouping (e.g., CHO, CHON) were then calculated as the sum of all the relative abundances of all the peaks in each compound class divided by the sum of all the assigned formulae abundances in each sample. For all mass spectra presented herein, 9,704–14,974 peaks were assigned elemental compositions with root-mean-square mass measurement accuracy for samples ranging from 36 to 48 ppb (Table S1 in Supporting Information S1).

3.6. Statistical Analyses

The experimental samples that were incubated and analyzed in triplicate (i.e., DOC concentrations and CDOM after 26 and 90 days) were averaged before any statistical analyses. Therefore, the standard error values reported represent variability among samples that were collected at different locations rather than experimental replicates. To test differences in bulk metrics between horizons, we first assessed normality of data using the Shapiro-Wilk test and the homogeneity of variance across groups using Levene's test. For variables that passed both tests

Table 1
Bulk Characteristics of Active Layer (AL), Holocene Terrestrial Permafrost (TP), and Pleistocene Marine Permafrost (MP) Samples

Horizon	Depth (cm)	TOC (%)	Leaching yield (mg-DOC gdw^{-1})	Leaching yield (mg-DOC g^{-1} TOC)	$BDOC_{26}$ (%)	$BDOC_{90}$ (%)	$S_{275-295}$ ($nm^{-1} \times 10^2$)	S_R	$SUVA_{254}$ (L mg^{-1} m^{-1})	*n*
AL	29 ± 1	11 ± 2	0.27 ± 0.07	2.4 ± 0.4	9.0 ± 3	23 ± 5	1.5 ± 0.03	0.82 ± 0.02	1.5 ± 0.2	6
TP	62 ± 3	11 ± 0.4	0.70 ± 0.02	6.3 ± 0.4	9.1 ± 2	14 ± 3	1.5 ± 0.09	0.77 ± 0.04	1.7 ± 0.3	3
MP	260 ± 12	1.7 ± 0.3	0.043 ± 0.004	2.7 ± 0.7	26 ± 5	33 ± 6	1.5 ± 0.3	1.2 ± 0.1	1.3 ± 0.3	3

Note. All reported values are mean ± standard error. Sample depth (cm from tundra surface), Total Organic Carbon content (TOC; %), Dissolved Organic Carbon leaching yields normalized to dry weight (mg-DOC gdw^{-1}) and to TOC content (mg-DOC g^{-1}-TOC), biodegradable DOC in leachates after 26 and 90 days incubations ($BDOC_{26}$, $BDOC_{90}$), and Chromophoric Dissolved Organic Matter indices of initial leachate DOM ($S_{275-295}$, S_R, $SUVA_{254}$).

($p > 0.05$), we assessed differences between horizons using a one-way ANOVA followed by a Tukey Honest Significant Differences post hoc test. For variables that failed the Shapiro-Wilk test ($p < 0.05$), we assessed differences between horizons using Kruskal-Wallis rank sum tests followed by Wilcoxon post hoc tests. For variables that passed the Kruskal-Wallis test but failed Levene's test, we assessed differences between horizons using the Welch One-Way ANOVA test followed by Games Howell post-hoc tests.

Principal component analysis (PCA) was used to examine relationships between DOM characteristics such as BDOC, %RA of compound classes, and CDOM parameters; these variables were scaled to unit variance. Spearman's rank correlation coefficients were used to examine how DOC leaching yields and BDOC were related to %RA of compound classes and other compositional metrics from FT-ICR MS analysis of DOM. Coefficients were reported if they had an absolute value Spearman's rank correlation coefficient $|(\rho)| > 0.2$ and a *p*-value < 0.05. To examine which DOM molecular formulae were associated with biodegradability, we calculated Spearman's rank correlation coefficients between BDOC at 26 days ($BDOC_{26}$; %) and peak intensity of each molecular formulae. These *p*-values were adjusted using a false discovery rate correction, and correlations with adjusted *p*-values < 0.05 were selected for analysis. Statistical analyses were completed using the "rstatix" v.0.7.0 (Kassambara, 2021), "Hmisc" v.4.6.0 (Harrell, 2021), and R Statistical Software v.4.1.3 (R Core Team, 2022). Additionally, "tidyverse" (Wickham et al., 2019) v.1.3.1 and "ggfortify" v. 0.4.14 (Horikoshi & Tang, 2016) packages were used to process and visualize the data.

4. Results and Discussion

4.1. Dissolved Organic Carbon Leaching Yields

Active layer soils and Holocene terrestrial permafrost had high TOC content (~11%) compared to Pleistocene marine permafrost (~1.7%; Figure 1 and Table 1). DOC leaching yields after 24 hr in seawater were statistically different between horizons when normalized to dry weight (Welch, $p < 0.0001$) and when normalized to TOC content (ANOVA, $p < 0.001$; Figure 3). When normalized to dry weight, Holocene terrestrial permafrost leached the most DOC (0.70 ± 0.02 mg-DOC gdw^{-1}), followed by active layer soils (0.27 ± 0.07 mg-DOC gdw^{-1}) and Pleistocene marine permafrost (0.043 ± 0.004 mg-DOC gdw^{-1}); each of these horizons was notably different from the other two (Games-Howell, $p < 0.05$). When normalized to TOC, Holocene terrestrial permafrost leached much more DOC (6.3 ± 0.4 mg-DOC g^{-1} TOC) than active layer (2.4 ± 0.4 mg-DOC g^{-1} TOC) and Pleistocene marine permafrost (2.7 ± 0.7 mg-DOC g^{-1} TOC; Tukey, $p < 0.01$).

Previous studies of DOC leaching from permafrost in seawater are very limited. To our knowledge, only one study to date has examined DOC yield from permafrost in seawater. Using tundra soils and permafrost near Elson Lagoon on the western Beaufort Sea, Dou et al. (2008) observed that seawater significantly reduced DOC yields compared to pure water. Similar to our results, upper permafrost samples near Elson Lagoon released more DOC compared to overlying active layer soils sampled at similar depths as in our study (Dou et al., 2008). Inland studies from Arctic Alaska showed that ~2% or less of total permafrost OC was released as DOC when freeze dried soils were shaken in freshwater (Gao et al., 2018; Guo et al., 2007; Xu et al., 2009). Our DOC leaching yields were <1% of total OC, but these extractions were performed gently on soils over a short time period and are therefore a

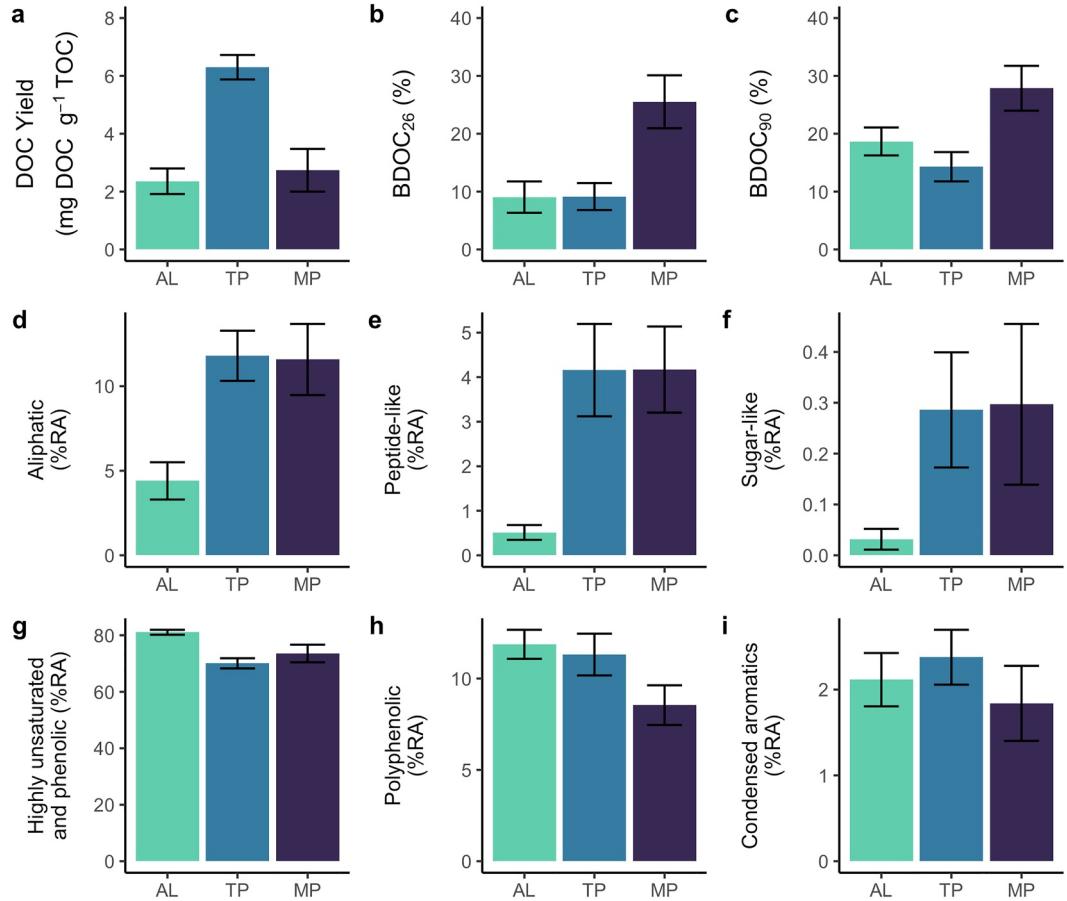

Figure 3. Characteristics of dissolved organic matter leached from active layer soils (AL; $n = 6$), Holocene terrestrial permafrost (TP; $n = 3$), and Pleistocene marine-derived permafrost (MP; $n = 3$). (a) dissolved organic carbon (DOC) leaching yield normalized by total organic carbon, (b) biodegradable DOC over 26 days, (c) biodegradable DOC over 90 days, (d) aliphatic formulae (%RA), (e) peptide-like formulae (%RA), (f) sugar-like formulae (%RA), (g) highly unsaturated and phenolic formulae (%RA), (h) polyphenolic formulae (%RA), and (i) condensed aromatic formulae (%RA).

conservative estimate of the DOC yield in the nearshore environment, where eroded material could be leached for months in turbulent shallow waters.

4.2. Biodegradable Dissolved Organic Carbon

Biodegradable DOC (BDOC; i.e., percent loss of DOC throughout the dark incubation) was clearly different between horizons after 26 days (ANOVA, $p = 0.01$; Table 1 and Figure 3) but less distinct after 90 days (ANOVA, $p = 0.1$). After 26 days, an average 26 ± 5% of DOC from Pleistocene marine permafrost was consumed, which was more than twice the active layer (9.0 ± 3%; Tukey, $p = 0.1$) and Holocene terrestrial permafrost (9.1 ± 2%; Tukey, $p = 0.03$). While active layer and Holocene terrestrial permafrost had similar BDOC after 26 days, by 90 days, BDOC leached from the active layer (23 ± 5%) was intermediate to Pleistocene marine permafrost (33 ± 6%) and Holocene terrestrial permafrost (14 ± 3%).

While many studies have used bottle incubation experiments to examine the biodegradability of DOC from inland permafrost and waterways (see meta-analysis by Vonk et al., 2015), this is the first of such studies to measure DOC losses from coastal permafrost leached in seawater. One relevant study from the western Canadian Arctic used a chemostat system to compare bacterial growth efficiency in DOC leached from three distinct deposits (Bruhn et al., 2021). While we cannot directly compare our results due to the different methods used, Bruhn et al. observed variable bacterial growth efficiencies, with higher utilization of DOC leached from moraine deposits and lower utilization of DOC leached from lacustrine and fluvial deposits (2021). Our BDOC measurements from coastal permafrost DOM in seawater are within the range of values observed from incubations of fresh soil

Table 2
Molecular Composition of Dissolved Organic Matter Leached from Active Layer (AL), Holocene Terrestrial Permafrost (TP), and Pleistocene Marine Permafrost (MP) Leachates as Measured by FT-ICR MS

Horizon	Mass (Da)	AI_{mod}	Cond. aromatics (%RA)	Polyphenolic (%RA)	Highly unsaturated and phenolic (%RA)	Aliphatic (%RA)	Peptide-like (%RA)	Sugar-like (%RA)	CHO (%RA)	CHON (%RA)	CHONS (%RA)	CHOS (%RA)
AL	531 ± 6	0.31 ± 0.01	2.1 ± 0.3	12 ± 0.8	81 ± 0.9	4.4 ± 1	0.51 ± 0.2	0.032 ± 0.02	67 ± 0.6	24 ± 2	0.67 ± 0.2	7.4 ± 0.9
TP	515 ± 6	0.28 ± 0.01	2.4 ± 0.3	11 ± 1	70 ± 2	12 ± 1	4.2 ± 1	0.29 ± 0.1	63 ± 0.2	24 ± 0.6	1.1 ± 0.1	12 ± 0.6
MP	501 ± 8	0.25 ± 0.01	1.8 ± 0.4	8.5 ± 1	74 ± 3	12 ± 2	4.2 ± 1	0.3 ± 0.2	60 ± 1	27 ± 1	2 ± 0.5	11 ± 2

Note. Relative intensity weighted average mass (mass), modified aromaticity index (AI_{mod}), and percent relative abundance (%RA) of compounds from FT-ICR MS analysis of DOM leached from active layer (n = 6), Holocene terrestrial permafrost (n = 3), and Pleistocene marine permafrost (n = 3). All reported values are mean ± standard error.

leachates and inland waters in permafrost regions (Vonk et al., 2015). BDOC in Pleistocene marine permafrost leachates from Drew Point was within the range of BDOC values measured from thermokarst features on the North Slope of Alaska (~10–60% over 40 days; Abbott et al., 2014) or from North Slope rivers during the spring freshet (~20–40% over 3 months; Holmes et al., 2008), but was less biodegradable than DOC from late-Pleistocene Siberian permafrost (~40–60% over 28 days; Spencer et al., 2015; Vonk et al., 2013). Our leachate BDOC measurements were also within the range measured from soil and permafrost leachates from Interior Alaska (9–45% over 28 days; Textor et al., 2019), active layer and permafrost porewater from the Yukon Coastal Plain (5%–17% over 21 days; Speetjens et al., 2022), and supra-permafrost groundwater sampled from Beaufort Sea coastal soils (3%–19% over 28 days; Bristol, 2023; Connolly, 2019). While our coastal active layer and Holocene terrestrial permafrost leachates had lower BDOC compared to some inland permafrost leachates, losses were greater than observed in northern Alaskan rivers during the summer season (Holmes et al., 2008), indicating coastal erosion as a potentially important source of BDOC to the Arctic Ocean during the summer.

4.3. Composition of Leachate Dissolved Organic Matter

CDOM revealed some differences in the bulk DOM leached from the three horizons (Table 1). $S_{275–295,}$ a proxy for molecular weight (Helms et al., 2008), was remarkably similar between horizons. However, S_R, which is inversely related to molecular weight and aromaticity (Helms et al., 2008; Spencer et al., 2012), was variable across horizons (Kruskal-Wallis, $p = 0.03$) with Pleistocene marine permafrost leachates having the highest S_R (1.2 ± 0.1) and Holocene terrestrial permafrost having the lowest (0.77 ± 0.04). S_R results likely reflect the different origins of OM, as the Pleistocene permafrost at Drew Point contains marine-derived OM (e.g., phytoplankton) that tends to be lower molecular weight and less aromatic compared to terrestrial OM derived from vascular plants (Hansen et al., 2016; Helms et al., 2008). $SUVA_{254}$, which is positivity correlated with aromaticity (Weishaar et al., 2003), was not clearly different between horizons (ANOVA, $p = 0.8$). In general, higher molecular weight and/or highly aromatic DOM with lower slopes, lower slope ratios and/or higher $SUVA_{254}$ values are expected to be more stable in the environment (Hansen et al., 2016). Except for $SUVA_{254}$ values, which were lower than typically observed in Arctic rivers, these CDOM indices are within the ranges commonly reported for porewater, soil leachates, streams, and rivers across the Arctic (Behnke et al., 2021; Gao et al., 2018; MacDonald et al., 2021; Speetjens et al., 2022).

Percent relative abundance (%RA) of formulae in assigned FT-ICR MS compound classes revealed more distinct compositional differences between horizons (Figure 3; Table 2). The %RA of aliphatic, peptide-like, and highly unsaturated and phenolic compounds in leached DOM were markedly different between horizons (ANOVA, $p < 0.01$). DOM leached from permafrost had a higher %RA of aliphatic and peptide-like compounds compared to DOM leached from active layer soils (Tukey, $p < 0.05$), and the permafrost horizons were similar to each other. While sugar-like formulae were a small fraction of formulae detected, there were also notable relationships suggesting that the two permafrost horizons had a higher %RA of sugar-like formulae compared to active layer leachates (Kruskal-Wallis $p = 0.06$). These aliphatic, peptide-like (i.e., N-containing aliphatic), and sugar-like

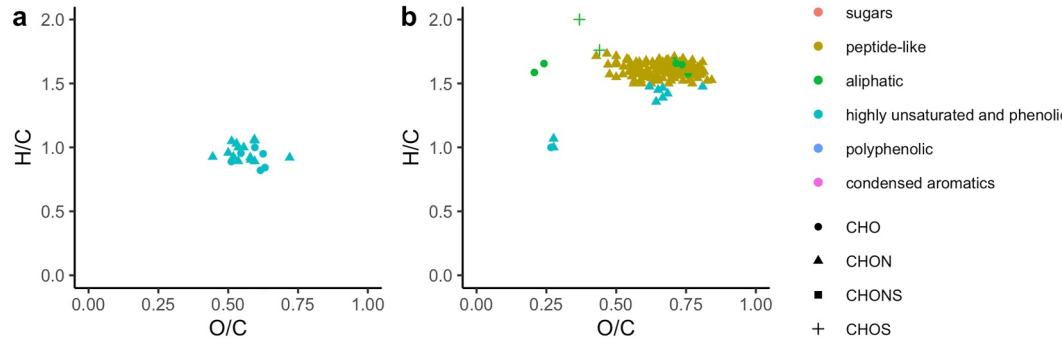

Figure 4. Unique molecular formulae leached from (a) active layer soils ($n = 6$) and (b) permafrost ($n = 6$). All formulae detected in the seawater control were removed from leachate dissolved organic matter pools prior to analysis of unique molecular formulae. Colors indicate the compound class of each formula, and symbols indicate if the compound contains nitrogen and/or sulfur.

compound classes are typically associated with bioavailable formulae that are preferentially utilized by microbial communities (D'Andrilli et al., 2015, 2023; Spencer et al., 2015; Textor et al., 2019). Compared to both permafrost horizons, the active layer had a higher %RA of highly unsaturated and phenolic compounds (Tukey, $p < 0.05$). The highly unsaturated and phenolic compound class contains aromatic compounds such as lignins and tannins derived from vascular plants, and aquatic carboxyl-rich alicyclic molecules that tend to be chemically stable (Behnke et al., 2021; D'Andrilli et al., 2015; Hertkorn et al., 2006; Kellerman et al., 2018). Similarly, we also detected differences in modified aromaticity index (AI_{mod}; ANOVA, $p = 0.01$), which was higher in the active layer compared to Pleistocene marine permafrost (Tukey, $p = 0.01$). The %RA of formulae without heteroatoms (i.e., CHO; formulae without nitrogen or sulfur) also varied between horizons (ANOVA, $p < 0.001$), with active layer DOM containing the highest %RA of molecular formulae without heteroatoms (Tukey, $p < 0.01$). Active layer leachates contained less nitrogen and sulfur containing compounds (CHONS; %RA) compared to Pleistocene marine permafrost (Tukey, $p = 0.02$). Additionally, there were weaker relationships suggesting that the active layer contains fewer sulfur containing compounds (CHOS; %RA) compared to Holocene terrestrial permafrost (Tukey, $p = 0.07$) and Pleistocene marine permafrost (Tukey, $p = 0.08$). Together, these results suggest that active layer leachates contain relatively more aromatic formulae, whereas the permafrost leachates contain relatively more aliphatic molecular formulae and heteroatom-containing molecular formulae.

The permafrost leachates contained a high %RA of aliphatic (~12%) and peptide-like (~4%) molecular formulae compared to DOM from pan-Arctic streams, rivers, and lakes (Behnke et al., 2021; Johnston et al., 2018, 2021; Kurek et al., 2023; Textor et al., 2019; Wologo et al., 2021). For example, in a multiyear study of six major Arctic Rivers across seasons, %RA of aliphatic and peptide-like compounds averaged only ~4–6% and 0.3%–0.7% respectively, using the same 21T FT-ICR MS and methodology as utilized in this study (Behnke et al., 2021). DOM leached from active layer soils was more similar to surface water inputs to the Arctic Ocean, likely reflecting transport of active layer DOM to surface waters via supra-permafrost groundwater flow (Behnke et al., 2021; Connolly et al., 2020). Likewise, the DOM leached from the active layer in our experiments was remarkably similar in composition to supra-permafrost groundwater DOM sampled from Beaufort Sea coastal soils during summer (Bristol, 2023; Connolly, 2019). The higher %RA of aliphatic and peptide-like molecular formulae observed in permafrost leachates compared to active layer leachates likely accumulated from slow microbial processing over thousands of years in anoxic frozen soils (Antony et al., 2017; Hodgkins et al., 2016; Musilova et al., 2017). Other studies have also shown that permafrost-derived DOM contains relatively more aliphatic compounds than overlaying active layer soils, consistent with our observations (MacDonald et al., 2021; Ward & Cory, 2015).

To further investigate the differences in DOM composition across horizons, we examined individual molecular formulae that were unique to active layer soil leachates versus permafrost (Figure 4). "Unique" formulae were defined as molecular formulae that were detected in all leachates within a category but were not detected in any other leachates. This analysis resulted in similar patterns to the compound class %RA comparisons. Formulae unique to active layer leachates were highly unsaturated and phenolic compounds with lower average H/C ratios (0.95 ± 0.02) compared to permafrost leachates (1.60 ± 0.01). Additionally, most unique formulae leached from

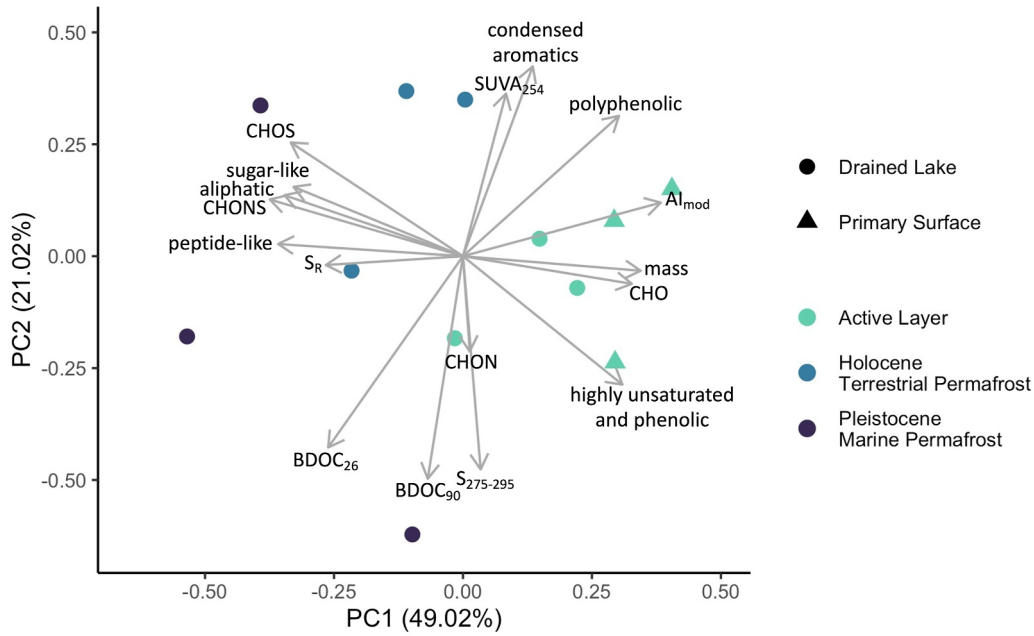

Figure 5. Principal components analysis of leached dissolved organic matter (DOM) characteristics including relative abundance (%) of compound classes, relative intensity weighted average mass (mass), modified aromaticity index (AI_{mod}), biodegradable dissolved organic carbon at 26 ($BDOC_{26}$) and 90 days ($BDOC_{90}$), and chromophoric dissolved organic matter indices (i.e., $S_{275–295}$, S_R, $SUVA_{254}$). Color indicates the horizon DOM was leached from and symbols indicate the surface geomorphology.

permafrost contained nitrogen and were categorized as peptide-like. Interestingly, there were more formulae unique to all six permafrost leachates (168 formulae; Figure 4) than unique to the sub-classifications of Holocene terrestrial permafrost (53 formulae) and Pleistocene marine permafrost (27 formulae; Figure S1 in Supporting Information S1).

The compositional similarity of DOM leached from Holocene terrestrial and Pleistocene marine permafrost is somewhat surprising. Since the origins of OM in the two permafrost horizons are distinct (i.e., terrestrial/lacustrine vs. marine), these analyses of leached DOM suggests that a notable fraction of formulae in permafrost are produced by microbial or physical processing in conditions unique to permafrost, rather than originating from the parent source of OM. We hypothesize that aliphatic and peptide-like compounds are formed by microbial activity in anoxic permafrost soils (Ewing et al., 2015; Heslop et al., 2019; Leewis et al., 2020), although lacustrine and marine primary production may also be a source of biolabile, aliphatic OM to permafrost horizons (D'Andrilli et al., 2015). Other studies have demonstrated that permafrost soils contain a higher abundance of low molecular weight, oxygen-poor, and aliphatic compounds relative to overlaying active layer soils (MacDonald et al., 2021; Textor et al., 2019; Ward & Cory, 2015). Previous studies of Yedoma permafrost show the prevalence of highly biolabile, low molecular weight organic acids accumulate from incomplete anerobic decomposition of OM over thousands of years (Drake et al., 2015; Ewing et al., 2015; Heslop et al., 2019). We hypothesize that aliphatic and peptide-like formulae that are more abundant or unique to permafrost slowly accumulate from anerobic microbial activity in frozen permafrost and these formulae can rapidly be decomposed in aerobic conditions following permafrost thaw. We also note that permafrost leachate DOM had a higher %RA of sulfur-containing formulae (Table 2), which may reflect redox conditions in permafrost (Lau & Del Giorgio, 2020).

4.4. Relationships Between Dissolved Organic Matter Composition and Biodegradability

Principal component analysis (PCA) of the leachate samples largely corroborated our comparisons of compound classes between horizons, with samples grouping together by layer (Figure 5). Active layer and permafrost samples clearly separated along PC1, which explained 49% of the data variance. Active layer leachates separated on the positive end of PC1, which correlated with AI_{mod}, molecular weight, CHO, and highly unsaturated and phenolic compounds. Sugar-like, aliphatic, CHONS, and peptide-like compounds were negatively related to PC1,

Table 3
Spearman's Correlations ($|\rho| > 0.2$; $p < 0.05$) Between Leaching Yields (mg-DOC g^{-1} Total Organic Carbon), Biodegradable Dissolved Organic Carbon (DOC) After 26 days ($BDOC_{26}$), Biodegradable DOC After 90 days ($BDOC_{90}$) and Dissolved Organic Matter Compositional Metrics From FT-ICR MS

	Mass (Da)	AI_{mod}	Condensed aromatics (%RA)	Polyphenolic (%RA)	Highly unsaturated and phenolic (%RA)	Aliphatic (%RA)	Peptide-like (%RA)	Sugar-like (%RA)	CHO (%RA)	CHON (%RA)	CHONS (RA)	CHOS (%RA)
Leaching yield	–	–	–	–	−0.58	–	0.38	0.50	–	–	–	0.25
$BDOC_{26}$	−0.56	−0.76	−0.72	−0.80	−0.22	0.52	0.55	0.36	−0.43	–	0.48	0.29
$BDOC_{90}$	–	−0.33	−0.52	−0.50	–	–	–	–	–	0.35	–	–

corresponding to the Pleistocene marine permafrost leachates. Holocene terrestrial permafrost generally grouped between the other two horizons, possibly reflecting similarities in OM source with the active layer and similarities in diagenic processing with the Pleistocene marine permafrost. In addition to showing these compositional differences between horizons, the PCA provided insight on how DOM biodegradability relates to chemical composition. BDOC at both timepoints fell along PC2, which explained 21% of the variability. CHON (%RA), $BDOC_{90}$, and $S_{275–295}$ were strongly negatively related to PC2, and and $SUVA_{254}$ and condensed aromatics were strongly positively related to PC2. $BDOC_{26}$ was negatively related to PC2 and, to a lesser extent, negatively related to PC1. The PCA thus supported the high %RA of peptide-like, aliphatic, sugar-like, and sulfur containing formulae in permafrost. However, PC2 added greater nuance with respect to the drivers of DOM biodegradability; the separation along PC2 suggests that leachates with lower molecular weight DOM, higher %RA of nitrogen-containing formulae, and fewer aromatic and polyphenolic formulae are more biodegradable, particularly after the longer incubation period.

Spearman rank correlation coefficients further reveal how leaching yields and BDOC are related to the composition of DOM (Table 3). DOC leaching yields were positively correlated with %RA of peptide-like and sugar-like compounds and negatively related to %RA of highly unsaturated and phenolic compounds. As suggested by the PCA $BDOC_{26}$ was negatively related with unsaturated and aromatic compound classes and positively related with saturated compound classes (i.e., aliphatic, peptide-like, sugar-like). While $BDOC_{26}$ had more significant correlations than $BDOC_{90,}$ the patterns were similar. These relationships are also supported by CDOM data. BDOC at both timepoints was positively correlated with initial leachate $S_{275–295}$ and S_R and negatively correlated with $SUVA_{254}$ (Table S2 in Supporting Information S1), indicating that lower molecular weight (Helms et al., 2008) and less aromatic (Weishaar et al., 2003) DOM was more easily used by microbial communities. Furthermore, $SUVA_{254}$ generally increased throughout the BDOC incubations (Figure S3 in Supporting Information S1), which reflects the preferential consumption of less aromatic compounds by microbial communities.

Spearman correlations were also used to investigate which individual formulae, as detected by FT-ICR MS, were correlated with biodegradability (Figure 6). Combining results from all leachates, we did not detect any correlations (p-adj < 0.05) between $BDOC_{26}$ or $BDOC_{90}$ and peak intensity of individual formulae, which is unsurprising given the apparent chemical differences between permafrost and active layer samples and thus the likelihood that different formulae are bioavailable in each sample type. Within just the permafrost leachates, however, the formulae that were strongly positively correlated with $BDOC_{26}$ were typically nitrogen containing formulae with H/C > 1.0. Formulae that were strongly negatively correlated with $BDOC_{26}$ had H/C < 1.0 and did not contain nitrogen. Previous work linking BDOC experiments with FT-ICR MS compositional data show similar results, where formulae with higher H/C ratios (i.e., aliphatic, sugar-like, peptide-like compound classifications) are more biolabile and quickly decomposed across a wide range of DOM sources including vegetation leachates, freshwaters, and soils sampled globally (D'Andrilli et al., 2015, 2023). Formulae with high H/C are also linked to BDOC in focused studies of high latitude environments, including studies of DOM from permafrost-influenced streams and rivers, as well as vegetation, soil, and permafrost leachates (Spencer et al., 2015; Textor et al., 2019). However, our latter timepoint ($BDOC_{90}$) incubation results indicated that DOM pools with a higher %RA of nitrogen containing formulae and lower %RA of condensed aromatic and polyphenolic compounds were more biodegradable on longer time scales (Table 3, Figure 5). This is consistent with previous work that suggests that phenolic and aromatic compounds are generally stable and may even inhibit

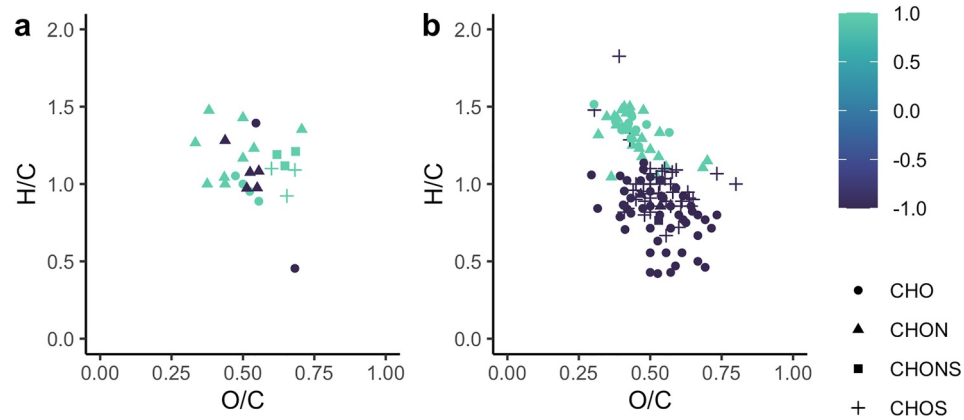

Figure 6. Subset of individual molecular formulae in panels (a) active layer soils and (b) permafrost that had strong Spearman rank correlation coefficients ($p_{adj} < 0.05$) between the peak intensity of individual molecular formula and $BDOC_{26}$ (%). All formulae with $p_{adj} < 0.05$ had Spearman ρ of 1 or −1, indicating perfect monotonic relationships between peak intensity and biodegradable dissolved organic carbon. Spearman rank correlation coefficients are indicated by the color scale, with light colors signifying positive correlations and dark colors signifying negative correlations. Symbols indicate if formulae contain nitrogen and/or sulfur.

microbial activity (D'Andrilli et al., 2015; Mann et al., 2014; Ward & Cory, 2015). Linkages between the %RA of nitrogen containing formulae and BDOC has also been shown in a study of supra-permafrost groundwater and surface waters along the Alaska Beaufort Sea coast (Bristol, 2023). We hypothesize that aliphatic compounds are quickly consumed, driving differences in BDOC on shorter timescales. BDOC on longer timescales is better predicted by higher abundance of nitrogen-containing compounds and lower relative abundance of highly aromatic compounds, which are a larger proportion of the initial DOM pool.

Although FT-ICR MS analysis revealed many similarities between DOM leached from the two permafrost horizons, Holocene terrestrial permafrost had significantly lower BDOC than Pleistocene marine permafrost (Figure 3). This may be partially attributed to the greater %RA of aromatic and polyphenolic formulae and lower %RA of nitrogen-containing formulae in Holocene terrestrial permafrost, characteristic of more stable, terrestrially derived OM (Figure 3, Table 2). It may also be that the aliphatic and peptide-like formulae unique to permafrost DOM in this study (Figures 4 and 5) are a small fraction of the DOM pool. We also acknowledge that the microbial communities present in soil/sediments and/or that developed during the bottle incubations could impact decomposition rates. One hypothesis is that the microbial community in seawater is better suited to utilize marine-derived OM (Grevesse et al., 2022; Logue et al., 2016; Underwood et al., 2019) due to its greater availability in the marine environment. Since marine-derived permafrost has porewater salinity values that approach seawater (Bristol et al., 2021), it is possible that salt tolerant microbes in the sediment inoculated the seawater, leading to more rapid DOC consumption in the first timepoint ($BDOC_{26}$) relative to the terrestrial soil leachates. It is also possible that discrimination during solid phase extraction and/or ion suppression during electrospray ionization led to underestimating the abundance of highly saturated carbohydrates or other biolabile compounds present in the leachates (Grasset et al., 2023; Hertkorn et al., 2013).

4.5. Scaling Leaching and Biodegradability Measurements

To scale the results of this experimental work, we combined our leaching and BDOC values with previously published measurements of TOC stocks in eroding bluffs at Drew Point, Alaska (Bristol et al., 2021). A typical 4 m bluff at Drew Point stores 98.8 kg TOC m^{-2}, with each horizon contributing a similar amount of OC to the total stock (Table 4). Assuming our experimental leaching rates from each horizon, we expect the Holocene terrestrial permafrost in an average bluff to contribute a higher portion of total DOC yields (~46%) compared to the other horizons following bluff collapse. However, when our BDOC results are considered, we predict the Pleistocene marine permafrost to contribute the most BDOC. Combining these data with high resolution measurements of modern (2008–2018) erosional TOC fluxes (12,297 Mg C yr^{-1}; Bristol et al., 2021), we predict that ~39 Mg yr^{-1} of DOC leaches from eroding material along this 9 km study coastline. This estimate is small compared to DOC inputs from the nearest river, the Colville, which is the largest river draining the North Slope

Table 4
Total Organic Carbon Stocks, Dissolved Organic Carbon Leaching Yields, and Biodegradable Dissolved Organic Carbon Yields From a Typical 4 m Bluff Eroding at Drew Point, Alaska

Horizon	Elevation (m)	TOC stock (kg TOC m^{-2})	DOC yield (g DOC m^{-2})	BDOC yield (g BDOC m^{-2})
Active Layer	3.6–4.0	39.9 (40%)	90.1 (26%)	21.7 (29%)
Holocene Terrestrial Permafrost	3.0–3.6	25.1 (25%)	157.9 (46%)	22.6 (30%)
Pleistocene Marine Permafrost	0–3.0	33.8 (34%)	92.6 (27%)	30.7 (41%)
Total	4	98.8	340.6	75.0

Note. Percent values in parentheticals represent the contribution of each horizons to the bluff. TOC stocks were calculated using data from Bristol et al. (2020, 2021). DOC yields were estimated using our 24 hr experimental leaching yields. BDOC was estimated using our $BDOC_{90}$ results.

(~120 Gg DOC yr^{-1}; McClelland et al., 2014). However, considering that Drew Point is over 100 km from the Colville, erosion is still likely an important source of DOM to local nearshore waters. Moreover, we predict that ~9.4 Mg (~24%) of the leached DOC can be decomposed in the coastal environment. This erosion-derived DOC is more biodegradable than typical summer and fall surface water DOC (Holmes et al., 2008; Wologo et al., 2021), likely related to the relatively high fraction of aliphatic and nitrogen containing compounds present in our leachates.

We also estimate DOC yields from soils eroding along the entire Alaska Beaufort Sea coast (1,957 km) using TOC flux estimates from Ping et al. (153 Gg OC yr^{-1}; 2011). Since marine-derived OC is not found in eroding permafrost across the entire coastline, we averaged our active layer and Holocene terrestrial permafrost leaching and BDOC values to estimate that approximately 662 Mg DOC quickly leaches from eroding soils. Of this leached DOC, we estimate that 123 Mg DOC can incorporated in biomass or decomposed. To compare this value to river inputs entering the Alaska Beaufort Sea during the open water season, we assume that ~40% of annual river discharge occurs during the summer and use average DOC concentrations from this season to estimate that the three largest rivers draining to the Alaska Beaufort Sea supply 32,820 Mg DOC during the summer (McClelland et al., 2014). About ~5% of summer riverine DOC, or 1,641 Mg DOC, is biodegradable (Holmes et al., 2008). While our estimates of BDOC leached from eroding soils are <10% of what major rivers supply during the open water season, this is a considerable amount of biolabile OM that has not been accounted for in previous assessments. These scaling exercises are conservative estimates of DOC yields, as we only measured DOC released over 24 hr in a laboratory setting with little agitation. Along Beaufort Sea coastlines with high erosion rates, there is substantial wave action that reworks sediments along the coastline. While leaching yield rates will diminish over time (Wickland et al., 2007), we expect higher DOC release from eroded soils over days or weeks in the nearshore environment. Additionally, improved erosion rate estimates along the Alaska Beaufort Sea (Gibbs & Richmond, 2017) are higher than estimated by Ping et al. (2011), so we are likely also underestimating TOC fluxes and therefore DOC release from eroding soils on the Beaufort Sea coast.

Even if annual erosion-derived DOC inputs are small in magnitude relative to surface water DOC fluxes to the ocean, the timing of these inputs may be ecologically significant to coastal Arctic food webs. Numerous studies along the Alaska Beaufort Sea coast have demonstrated that terrestrial OM supports multiple trophic levels, including benthic organisms, fish, and birds (Bell et al., 2016; Dunton et al., 2012; Harris et al., 2018; Stanek et al., 2022). During summer, however, the fluxes and the quality of riverine DOC are substantially lower than during the spring freshet (Behnke et al., 2021; Holmes et al., 2008, 2012; McClelland et al., 2014; Wickland et al., 2012). Additionally, declines in inorganic nutrient inputs and solar radiation following the freshet are associated with declines in autochthonous production (Connelly et al., 2015; Kellogg et al., 2019; McClelland et al., 2014). Previous work along the Beaufort Sea showed that, during this transition from spring to summer, planktonic lagoon food webs shift from being phototrophic to heterotrophic-dominated (Connelly et al., 2015; Kellogg et al., 2019). Therefore, leached DOM from eroded material may be an important energy subsidy for these detrital-based summer food webs, providing a fresh source of bioavailable DOM to consumers.

5. Conclusions

Our results demonstrate that DOC is rapidly leached from eroding active layer and permafrost soils in seawater, and that a considerable fraction of this leached DOC can be quickly decomposed or incorporated within microbial

biomass. We found that marine-derived permafrost OM was more biodegradable than terrestrially derived OM in seawater. However, FT-ICR MS data show that permafrost horizons of different origins leached similar aliphatic molecular formulae that were either not detected or less relatively abundant in active layer leachates, suggesting there are physical or chemical processes occurring within permafrost that alter DOM composition. Since both leaching and biodegradable DOC was relatively variable across horizons, future studies should focus on sampling additional sites and examining how landscape geomorphology and/or bulk geochemical measurements can be used to assess leaching and biodegradability across the coastline.

Although we estimate that eroded soils supply considerably less DOC than rivers along the Alaska Beaufort Sea coast, we hypothesize that erosion is an important source of BDOC to nearshore coastal waters where and when river inputs are low. We expect the relative importance of coastal erosion to be greater along sections of coastline that are far from large rivers and/or have high erosion rates, such as along the western Beaufort Sea (Figure 1). Perhaps more importantly, North Slope river discharge, DOC concentrations, and DOC biodegradability are high during the spring freshet in May or June, but rapidly decline thereafter (Holmes et al., 2008; McClelland et al., 2014). Coastal erosion primarily occurs later in the summer open water season (Irrgang et al., 2022), thereby leaching relatively fresh, biolabile DOC to coastal waters when biodegradable DOC inputs from rivers are low.

Data Availability Statement

Geochemical data including soil and permafrost leaching yields, biodegradability measurements, and summarized DOM composition data are available at Environmental Data Initiative (https://doi.org/10.6073/pasta/bffc3d4e9cdc255ff0e8582d668c006e; Bristol et al., 2024). Soil and permafrost data used to estimate total organic carbon stocks at Drew Point are available at Environmental Data Initiative (https://doi.org/10.6073/pasta/cc4d53a91ed873765224fcb6d09f5eb7; Bristol et al., 2020). Raw FT-ICR MS data files are available at Open Science Framework (https://doi.org/10.17605/OSF.IO/MD2YZ; McKenna et al., 2024).

Acknowledgments

Field work for this project was completed on traditional Iñupiat land. The authors would like to thank Ryan Hladniuk, Kaijun Lu, and Zhanfei Liu for assistance with laboratory analyses, and Louise Farquharson, Jennifer Frederick, and Matthew Thomas for assistance with field sampling. This work was supported by the Laboratory Directed Research and Development (LDRD) program at Sandia National Laboratories, a multimission laboratory managed and operated by National Technology and Engineering Solutions of Sandia LLC, a wholly owned subsidiary of Honeywell International Inc. for the U.S. Department of Energy's National Nuclear Security Administration under contract DE-NA0003525. Graduate student participation at the University of Texas at Austin (E.B.) was supported by an Academic Alliance Partnership plus-up on the LDRD project and NSF award 1938820. This work was also supported by the Beaufort Lagoon Ecosystems Long Term Ecological Research project (NSF award 1665026). BMJ was additionally supported through NSF awards OISE-1927553 and OPP-2336164. A portion of laboratory work was performed at the National High Magnetic Field Laboratory ICR User Facility, which is supported by the National Science Foundation Division of Chemistry and Division of Materials Research through DMR-1644779, DMR-2128556, and the State of Florida.

References

Abbott, B. W., Larouche, J. R., Jones, J. B., Bowden, W. B., & Balser, A. W. (2014). Elevated dissolved organic carbon biodegradability from thawing and collapsing permafrost. *Journal of Geophysical Research: Biogeosciences*, *119*(10), 2049–2063. https://doi.org/10.1002/2014JG002678

Antony, R., Willoughby, A. S., Grannas, A. M., Catanzano, V., Sleighter, R. L., Thamban, M., et al. (2017). Molecular insights on dissolved organic matter transformation by supraglacial microbial communities. *Environmental Science & Technology*, *51*(8), 4328–4337. https://doi.org/10.1021/acs.est.6b05780

Bahureksa, W., Borch, T., Young, R. B., Weisbrod, C. R., Blakney, G. T., & McKenna, A. M. (2022). Improved dynamic range, resolving power, and sensitivity achievable with FT-ICR mass spectrometry at 21 T reveals the hidden complexity of natural organic matter. *Analytical Chemistry*, *94*(32), 11382–11389. https://doi.org/10.1021/acs.analchem.2c02377

Beaufort Lagoon Ecosystem LTER. (2024). Dissolved organic carbon (DOC) and total dissolved nitrogen (TDN) from river, lagoon, and open ocean sites along the Alaska Beaufort Sea coast, 2018-ongoing (Version 9) [Dataset]. https://doi.org/10.6073/pasta/19238e820291124f806a4e8cc0393118

Behnke, M. I., McClelland, J. W., Tank, S. E., Kellerman, A. M., Holmes, R. M., Haghipour, N., et al. (2021). Pan-Arctic riverine dissolved organic matter: Synchronous molecular stability, shifting sources and subsidies. *Global Biogeochemical Cycles*, *35*(4). https://doi.org/10.1029/2020GB006871

Bell, L., Bluhm, B., & Iken, K. (2016). Influence of terrestrial organic matter in marine food webs of the Beaufort Sea shelf and slope. *Marine Ecology Progress Series*, *550*, 1–24. https://doi.org/10.3354/meps11725

Bristol, E. M. (2023). *Sources and fate of terrestrial organic matter in Arctic coastal waters* (Dissertation). The University of Texas at Austin.

Bristol, E. M., Behnke, M. I., Spencer, R. G. M., McKenna, A. M., Jones, B. M., Bull, D. L., & McClelland, J. W. (2024). Composition and biodegradability of dissolved organic matter leached from eroding coastal soils and permafrost in seawater, from Drew Point, Alaska (Version 1) [Dataset]. *Environmental Data Intitiative*. Composition and biodegradability of dissolved organic matter leached from eroding coastal soils and permafrost in seawater, from Drew Point, Alaska. https://doi.org/10.6073/pasta/bffc3d4e9cdc255ff0e8582d668c006e

Bristol, E. M., Connolly, C. T., Lorenson, T. D., Richmond, B. M., Ilgen, A. G., Choens, R. C., et al. (2020). Geochemical characterization and material properties of coastal permafrost near Drew Point, Alaska (Version 1) [Dataset]. *Environmental Data Intitiative*. https://doi.org/10.6073/pasta/cc4d53a91ed873765224fcb6d09f5eb7

Bristol, E. M., Connolly, C. T., Lorenson, T. D., Richmond, B. M., Ilgen, A. G., Choens, R. C., et al. (2021). Geochemistry of coastal permafrost and erosion-driven organic matter fluxes to the Beaufort Sea near Drew Point, Alaska. *Frontiers in Earth Science*, *8*, 598933. https://doi.org/10.3389/feart.2020.598933

Bruhn, A. D., Stedmon, C. A., Comte, J., Matsuoka, A., Speetjens, N. J., Tanski, G., et al. (2021). Terrestrial dissolved organic matter mobilized from eroding permafrost controls microbial community composition and growth in arctic coastal zones. *Frontiers in Earth Science*, *9*, 640580. https://doi.org/10.3389/feart.2021.640580

Connelly, T., McClelland, J., Crump, B., Kellogg, C., & Dunton, K. (2015). Seasonal changes in quantity and composition of suspended particulate organic matter in lagoons of the Alaskan Beaufort Sea. *Marine Ecology Progress Series*, *527*, 31–45. https://doi.org/10.3354/meps11207

Connolly, C. T. (2019). *Dissolved organic matter in Arctic watersheds and coastal waters* (Dissertation). The University of Texas at Austin. https://doi.org/10.26153/tsw/8210

Connolly, C. T., Cardenas, M. B., Burkart, G. A., Spencer, R. G. M., & McClelland, J. W. (2020). Groundwater as a major source of dissolved organic matter to Arctic coastal waters. *Nature Communications*, *11*(1), 1479. https://doi.org/10.1038/s41467-020-15250-8

Corilo, Y. E. (2015). *PetroOrg software*. Omics LLC.

D'Andrilli, J., Cooper, W. T., Foreman, C. M., & Marshall, A. G. (2015). An ultrahigh-resolution mass spectrometry index to estimate natural organic matter lability. *Rapid Communications in Mass Spectrometry*, *29*(24), 2385–2401. https://doi.org/10.1002/rcm.7400

D'Andrilli, J., Romero, C. M., Zito, P., Podgorski, D. C., Payn, R. A., Sebestyen, S. D., et al. (2023). Advancing chemical lability assessments of organic matter using a synthesis of FT-ICR MS data across diverse environments and experiments. *Organic Geochemistry*, *184*, 104667. https://doi.org/10.1016/j.orggeochem.2023.104667

Dinter, D. A., Carter, L. D., & Brigham-Grette, J. (1990). Late Cenozoic geologic evolution of the Alaskan North Slope and adjacent continental shelves. In A. Grantz, L. Johnson, & J. F. Sweeney (Eds.), *Geology of North America*, *The Arctic Ocean region* (Vol. L, pp. 459–490). Geological Society of America. https://doi.org/10.1130/DNAG-GNA-L.459

Dittmar, T., Koch, B., Hertkorn, N., & Kattner, G. (2008). A simple and efficient method for the solid-phase extraction of dissolved organic matter (SPE-DOM) from seawater: SPE-DOM from seawater. *Limnology and Oceanography: Methods*, *6*(6), 230–235. https://doi.org/10.4319/lom.2008.6.230

Dou, F., Ping, C.-L., Guo, L., & Jorgenson, T. (2008). Estimating the impact of seawater on the production of soil water-extractable organic carbon during coastal erosion. *Journal of Environmental Quality*, *37*(6), 2368–2374. https://doi.org/10.2134/jeq2007.0403

Drake, T. W., Guillemette, F., Hemingway, J. D., Chanton, J. P., Podgorski, D. C., Zimov, N. S., & Spencer, R. G. M. (2018). The ephemeral signature of permafrost carbon in an Arctic fluvial network. *Journal of Geophysical Research: Biogeosciences*, *123*(5), 1475–1485. https://doi.org/10.1029/2017JG004311

Drake, T. W., Wickland, K. P., Spencer, R. G. M., McKnight, D. M., & Striegl, R. G. (2015). Ancient low–molecular-weight organic acids in permafrost fuel rapid carbon dioxide production upon thaw. *Proceedings of the National Academy of Sciences*, *112*(45), 13946–13951. https://doi.org/10.1073/pnas.1511705112

Dunton, K. H., Schonberg, S. V., & Cooper, L. W. (2012). Food web structure of the Alaskan nearshore shelf and estuarine lagoons of the Beaufort Sea. *Estuaries and Coasts*, *35*(2), 416–435. https://doi.org/10.1007/s12237-012-9475-1

Ewing, S. A., O'Donnell, J. A., Aiken, G. R., Butler, K., Butman, D., Windham-Myers, L., & Kanevskiy, M. Z. (2015). Long-term anoxia and release of ancient, labile carbon upon thaw of Pleistocene permafrost. *Geophysical Research Letters*, *42*(24). https://doi.org/10.1002/2015GL066296

Gao, L., Zhou, Z., Reyes, A. V., & Guo, L. (2018). Yields and characterization of dissolved organic matter from different aged soils in northern Alaska. *Journal of Geophysical Research: Biogeosciences*, *123*(7), 2035–2052. https://doi.org/10.1029/2018JG004408

Gibbs, A. E., & Richmond, B. M. (2017). *National assessment of shoreline change—Summary statistics for updated vector shorelines and associated shoreline change data for the north coast of Alaska* (Report No. 2017–1107) (p. 21). U.S.-Canadian Border to Icy Cape. https://doi.org/10.3133/ofr20171107

Grasset, C., Groeneveld, M., Tranvik, L. J., Robertson, L. P., & Hawkes, J. A. (2023). Hydrophilic species are the most biodegradable components of freshwater dissolved organic matter. *Environmental Science & Technology*, *57*(36), 13463–13472. https://doi.org/10.1021/acs.est.3c02175

Grevesse, T., Guéguen, C., Onana, V. E., & Walsh, D. A. (2022). Degradation pathways for organic matter of terrestrial origin are widespread and expressed in Arctic Ocean microbiomes. *Microbiome*, *10*(1), 237. https://doi.org/10.1186/s40168-022-01417-6

Guo, L., Ping, C.-L., & Macdonald, R. W. (2007). Mobilization pathways of organic carbon from permafrost to arctic rivers in a changing climate. *Geophysical Research Letters*, *34*(13). https://doi.org/10.1029/2007GL030689

Hansen, A. M., Kraus, T. E. C., Pellerin, B. A., Fleck, J. A., Downing, B. D., & Bergamaschi, B. A. (2016). Optical properties of dissolved organic matter (DOM): Effects of biological and photolytic degradation: DOM optical properties following degradation. *Limnology & Oceanography*, *61*(3), 1015–1032. https://doi.org/10.1002/lno.10270

Harrell, F. (2021). Hmisc: Harrell miscellaneous. (Version 4.6-0). https://CRAN.R-project.org/package=Hmisc

Harris, C. M., McTigue, N. D., McClelland, J. W., & Dunton, K. H. (2018). Do high Arctic coastal food webs rely on a terrestrial carbon subsidy? *Food Webs*, *15*, e00081. https://doi.org/10.1016/j.fooweb.2018.e00081

Helms, J. R., Stubbins, A., Ritchie, J. D., Minor, E. C., Kieber, D. J., & Mopper, K. (2008). Absorption spectral slopes and slope ratios as indicators of molecular weight, source, and photobleaching of chromophoric dissolved organic matter. *Limnology & Oceanography*, *53*(3), 955–969. https://doi.org/10.4319/lo.2008.53.3.0955

Hendrickson, C. L., Quinn, J. P., Kaiser, N. K., Smith, D. F., Blakney, G. T., Chen, T., et al. (2015). 21 Tesla Fourier transform ion cyclotron resonance mass spectrometer: A national resource for ultrahigh resolution mass analysis. *Journal of the American Society for Mass Spectrometry*, *26*(9), 1626–1632. https://doi.org/10.1007/s13361-015-1182-2

Hertkorn, N., Benner, R., Frommberger, M., Schmitt-Kopplin, P., Witt, M., Kaiser, K., et al. (2006). Characterization of a major refractory component of marine dissolved organic matter. *Geochimica et Cosmochimica Acta*, *70*(12), 2990–3010. https://doi.org/10.1016/j.gca.2006.03.021

Hertkorn, N., Harir, M., Koch, B. P., Michalke, B., & Schmitt-Kopplin, P. (2013). High-field NMR spectroscopy and FTICR mass spectrometry: Powerful discovery tools for the molecular level characterization of marine dissolved organic matter. *Biogeosciences*, *10*(3), 1583–1624. https://doi.org/10.5194/bg-10-1583-2013

Heslop, J. K., Winkel, M., Walter Anthony, K. M., Spencer, R. G. M., Podgorski, D. C., Zito, P., et al. (2019). Increasing organic carbon biolability with depth in Yedoma permafrost: Ramifications for future climate change. *Journal of Geophysical Research: Biogeosciences*, *124*(7), 2021–2038. https://doi.org/10.1029/2018JG004712

Hinkel, K. M., Eisner, W. R., Bockheim, J. G., Nelson, F. E., Peterson, K. M., & Dai, X. (2003). Spatial extent, age, and carbon stocks in drained thaw lake basins on the Barrow Peninsula, Alaska. *Arctic Antarctic and Alpine Research*, *35*(3), 291–300. https://doi.org/10.1657/1523-0430(2003)035[0291:SEAACS]2.0.CO;2

Hodgkins, S. B., Tfaily, M. M., Podgorski, D. C., McCalley, C. K., Saleska, S. R., Crill, P. M., et al. (2016). Elemental composition and optical properties reveal changes in dissolved organic matter along a permafrost thaw chronosequence in a subarctic peatland. *Geochimica et Cosmochimica Acta*, *187*, 123–140. https://doi.org/10.1016/j.gca.2016.05.015

Holmes, R. M., McClelland, J. W., Peterson, B. J., Tank, S. E., Bulygina, E., Eglinton, T. I., et al. (2012). Seasonal and annual fluxes of nutrients and organic matter from large rivers to the Arctic Ocean and surrounding seas. *Estuaries and Coasts*, *35*(2), 369–382. https://doi.org/10.1007/s12237-011-9386-6

Holmes, R. M., McClelland, J. W., Raymond, P. A., Frazer, B. B., Peterson, B. J., & Stieglitz, M. (2008). Lability of DOC transported by Alaskan rivers to the Arctic Ocean. *Geophysical Research Letters*, *35*(3), L03402. https://doi.org/10.1029/2007GL032837

Horikoshi, M., & Tang, Y. (2016). ggfortify: Data visualization tools for statistical analysis results. Retrieved from https://CRAN.R-project.org/package=ggfortify

Irrgang, A. M., Bendixen, M., Farquharson, L. M., Baranskaya, A. V., Erikson, L. H., Gibbs, A. E., et al. (2022). Drivers, dynamics and impacts of changing Arctic coasts. *Nature Reviews Earth & Environment*, *3*(1), 39–54. https://doi.org/10.1038/s43017-021-00232-1

Johnston, S. E., Carey, J. C., Kellerman, A., Podgorski, D. C., Gewirtzman, J., & Spencer, R. G. M. (2021). Controls on riverine dissolved organic matter composition across an Arctic-boreal latitudinal gradient. *Journal of Geophysical Research: Biogeosciences*, *126*(9). https://doi.org/10.1029/2020JG005988

Johnston, S. E., Shorina, N., Bulygina, E., Vorobjeva, T., Chupakova, A., Klimov, S. I., et al. (2018). Flux and seasonality of dissolved organic matter from the northern Dvina (Severnaya Dvina) River, Russia. *Journal of Geophysical Research: Biogeosciences*, *123*(3), 1041–1056. https://doi.org/10.1002/2017JG004337

Jones, B. M., & Arp, C. D. (2015). Observing a catastrophic thermokarst lake drainage in northern Alaska. *Permafrost and Periglacial Processes*, *26*(2), 119–128. https://doi.org/10.1002/ppp.1842

Jones, B. M., Farquharson, L. M., Baughman, C. A., Buzard, R. M., Arp, C. D., Grosse, G., et al. (2018). A decade of remotely sensed observations highlight complex processes linked to coastal permafrost bluff erosion in the Arctic. *Environmental Research Letters*, *13*(11), 115001. https://doi.org/10.1088/1748-9326/aae471

Jones, B. M., Grosse, G., Farquharson, L. M., Roy-Léveillée, P., Veremeeva, A., Kanevskiy, M. Z., et al. (2022). Lake and drained lake basin systems in lowland permafrost regions. *Nature Reviews Earth & Environment*, *3*(1), 85–98. https://doi.org/10.1038/s43017-021-00238-9

Jones, M. C., Grosse, G., Jones, B. M., & Walter Anthony, K. (2012). Peat accumulation in drained thermokarst lake basins in continuous, ice-rich permafrost, northern Seward Peninsula, Alaska. *Journal of Geophysical Research*, *117*(G2). https://doi.org/10.1029/2011JG001766

Kassambara, A. (2021). rstatix: Pipe-friendly framework for basic statistical tests. (Version 0.7.2). https://CRAN.R-project.org/package=rstatix

Kellerman, A. M., Guillemette, F., Podgorski, D. C., Aiken, G. R., Butler, K. D., & Spencer, R. G. M. (2018). Unifying concepts linking dissolved organic matter composition to persistence in aquatic ecosystems. *Environmental Science & Technology*, *52*(5), 2538–2548. https://doi.org/10.1021/acs.est.7b05513

Kellogg, C. T. E., McClelland, J. W., Dunton, K. H., & Crump, B. C. (2019). Strong seasonality in Arctic estuarine microbial food webs. *Frontiers in Microbiology*, *10*, 2628. https://doi.org/10.3389/fmicb.2019.02628

Koch, B. P., & Dittmar, T. (2006). From mass to structure: An aromaticity index for high-resolution mass data of natural organic matter. *Rapid Communications in Mass Spectrometry*, *20*(5), 926–932. https://doi.org/10.1002/rcm.2386

Koch, B. P., & Dittmar, T. (2016). From mass to structure: An aromaticity index for high-resolution mass data of natural organic matter. *Rapid Communications in Mass Spectrometry*, *30*(1), 250. https://doi.org/10.1002/rcm.7433

Kurek, M. R., Garcia-Tigreros, F., Wickland, K. P., Frey, K. E., Dornblaser, M. M., Striegl, R. G., et al. (2023). Hydrologic and landscape controls on dissolved organic matter composition across western North American Arctic lakes. *Global Biogeochemical Cycles*, *37*(1), e2022GB007495. https://doi.org/10.1029/2022GB007495

Lau, M. P., & Del Giorgio, P. (2020). Reactivity, fate and functional roles of dissolved organic matter in anoxic inland waters. *Biology Letters*, *16*(2), 20190694. https://doi.org/10.1098/rsbl.2019.0694

Leewis, M.-C., Berlemont, R., Podgorski, D. C., Srinivas, A., Zito, P., Spencer, R. G. M., et al. (2020). Life at the frozen limit: Microbial carbon metabolism across a late Pleistocene permafrost chronosequence. *Frontiers in Microbiology*, *11*, 1753. https://doi.org/10.3389/fmicb.2020.01753

Logue, J. B., Stedmon, C. A., Kellerman, A. M., Nielsen, N. J., Andersson, A. F., Laudon, H., et al. (2016). Experimental insights into the importance of aquatic bacterial community composition to the degradation of dissolved organic matter. *The ISME Journal*, *10*(3), 533–545. https://doi.org/10.1038/ismej.2015.131

MacDonald, E. N., Tank, S. E., Kokelj, S. V., Froese, D. G., & Hutchins, R. H. S. (2021). Permafrost-derived dissolved organic matter composition varies across permafrost end-members in the western Canadian Arctic. *Environmental Research Letters*, *16*(2), 024036. https://doi.org/10.1088/1748-9326/abd971

Mann, P. J., Sobczak, W. V., LaRue, M. M., Bulygina, E., Davydova, A., Vonk, J. E., et al. (2014). Evidence for key enzymatic controls on metabolism of Arctic river organic matter. *Global Change Biology*, *20*(4), 1089–1100. https://doi.org/10.1111/gcb.12416

McClelland, J. W., Holmes, R. M., Dunton, K. H., & Macdonald, R. W. (2012). The Arctic Ocean estuary. *Estuaries and Coasts*, *35*(2), 353–368. https://doi.org/10.1007/s12237-010-9357-3

McClelland, J. W., Holmes, R. M., Peterson, B. J., Raymond, P. A., Striegl, R. G., Zhulidov, A. V., et al. (2016). Particulate organic carbon and nitrogen export from major Arctic rivers: POC and PN export from major Arctic rivers. *Global Biogeochemical Cycles*, *30*(5), 629–643. https://doi.org/10.1002/2015GB005351

McClelland, J. W., Townsend-Small, A., Holmes, R. M., Pan, F., Stieglitz, M., Khosh, M., & Peterson, B. J. (2014). River export of nutrients and organic matter from the North Slope of Alaska to the Beaufort Sea. *Water Resources Research*, *50*(2), 1823–1839. https://doi.org/10.1002/2013WR014722

McKenna, A. M., Behnke, M. I., & Bristol, E. M. (2024). P19500_Leaching and biolability of dissolved organic matter from eroding permafrost along the Alaska Beaufort Sea Coast [Dataset]. *Open Science Framework*. https://doi.org/10.17605/OSF.IO/MD2YZ

Musilova, M., Tranter, M., Wadham, J., Telling, J., Tedstone, A., & Anesio, A. M. (2017). Microbially driven export of labile organic carbon from the Greenland ice sheet. *Nature Geoscience*, *10*(5), 360–365. https://doi.org/10.1038/ngeo2920

Nielsen, D. M., Pieper, P., Barkhordarian, A., Overduin, P., Ilyina, T., Brovkin, V., et al. (2022). Increase in Arctic coastal erosion and its sensitivity to warming in the twenty-first century. *Nature Climate Change*, *12*(3), 263–270. https://doi.org/10.1038/s41558-022-01281-0

O'Donnell, J. A., Aiken, G. R., Butler, K. D., Guillemette, F., Podgorski, D. C., & Spencer, R. G. M. (2016). DOM composition and transformation in boreal forest soils: The effects of temperature and organic-horizon decomposition state. *Journal of Geophysical Research: Biogeosciences*, *121*(10), 2727–2744. https://doi.org/10.1002/2016JG003431

Ping, C.-L., Michaelson, G. J., Guo, L., Jorgenson, M. T., Kanevskiy, M., Shur, Y., et al. (2011). Soil carbon and material fluxes across the eroding Alaska Beaufort Sea coastline. *Journal of Geophysical Research*, *116*(G2), G02004. https://doi.org/10.1029/2010JG001588

R Core Team. (2022). *R: A language and environment for statistical computing* (Version 4.1.3). R Foundation for Statistical Computing. Retrieved from https://www.R-project.org/

Richardson, W. J., & Johnson, S. R. (1981). Waterbird migration near the Yukon and Alaskan Coast of the Beaufort Sea: I. Timing, routes and numbers in spring. *Arctic*, *34*(2), 108–121. https://doi.org/10.14430/arctic2512

Schell, D. M., Saupe, S. M., & Haubenstock, N. (1989). Bowhead whale (*Balaena mysticetus*) growth and feeding as estimated by 13C techniques. *Marine Biology*, *103*(4), 433–443. https://doi.org/10.1007/BF00399575

Smith, D. F., Podgorski, D. C., Rodgers, R. P., Blakney, G. T., & Hendrickson, C. L. (2018). 21 Tesla FT-ICR mass spectrometer for ultrahigh-resolution analysis of complex organic mixtures. *Analytical Chemistry*, *90*(3), 2041–2047. https://doi.org/10.1021/acs.analchem.7b04159

Speetjens, N. J., Tanski, G., Martin, V., Wagner, J., Richter, A., Hugelius, G., et al. (2022). Dissolved organic matter characterization in soils and streams in a small coastal low-Arctic catchment. *Biogeosciences*, *19*(12), 3073–3097. https://doi.org/10.5194/bg-19-3073-2022

Spencer, R. G. M., Butler, K. D., & Aiken, G. R. (2012). Dissolved organic carbon and chromophoric dissolved organic matter properties of rivers in the USA. *Journal of Geophysical Research*, *117*(G3). https://doi.org/10.1029/2011JG001928

Spencer, R. G. M., Mann, P. J., Dittmar, T., Eglinton, T. I., McIntyre, C., Holmes, R. M., et al. (2015). Detecting the signature of permafrost thaw in Arctic rivers. *Geophysical Research Letters*, *42*(8), 2830–2835. https://doi.org/10.1002/2015GL063498

Stanek, A. E., von Biela, V. R., Laske, S. M., Taylor, R. L., & Dunton, K. H. (2022). Barrier islands influence the assimilation of terrestrial energy in nearshore fishes. *Estuarine, Coastal and Shelf Science*, *278*, 108094. https://doi.org/10.1016/j.ecss.2022.108094

Tank, S. E., Manizza, M., Holmes, R. M., McClelland, J. W., & Peterson, B. J. (2012). The processing and impact of dissolved riverine nitrogen in the Arctic Ocean. *Estuaries and Coasts*, *35*(2), 401–415. https://doi.org/10.1007/s12237-011-9417-3

Tanski, G., Bröder, L., Wagner, D., Knoblauch, C., Lantuit, H., Beer, C., et al. (2021). Permafrost carbon and CO2 pathways differ at contrasting coastal erosion sites in the Canadian Arctic. *Frontiers in Earth Science*, *9*, 630493. https://doi.org/10.3389/feart.2021.630493

Tanski, G., Wagner, D., Knoblauch, C., Fritz, M., Sachs, T., & Lantuit, H. (2019). Rapid CO2 release from eroding permafrost in seawater. *Geophysical Research Letters*, *46*(20), 11244–11252. https://doi.org/10.1029/2019GL084303

Terhaar, J., Lauerwald, R., Regnier, P., Gruber, N., & Bopp, L. (2021). Around one third of current Arctic Ocean primary production sustained by rivers and coastal erosion. *Nature Communications*, *12*(1), 169. https://doi.org/10.1038/s41467-020-20470-z

Textor, S. R., Wickland, K. P., Podgorski, D. C., Johnston, S. E., & Spencer, R. G. M. (2019). Dissolved organic carbon turnover in permafrost-influenced watersheds of interior Alaska: Molecular insights and the priming effect. *Frontiers in Earth Science*, *7*, 275. https://doi.org/10.3389/feart.2019.00275

Underwood, G. J. C., Michel, C., Meisterhans, G., Niemi, A., Belzile, C., Witt, M., et al. (2019). Organic matter from Arctic sea-ice loss alters bacterial community structure and function. *Nature Climate Change*, *9*(2), 170–176. https://doi.org/10.1038/s41558-018-0391-7

Vonk, J. E., Mann, P. J., Davydov, S., Davydova, A., Spencer, R. G. M., Schade, J., et al. (2013). High biolability of ancient permafrost carbon upon thaw. *Geophysical Research Letters*, *40*(11), 2689–2693. https://doi.org/10.1002/grl.50348

Vonk, J. E., Tank, S. E., Mann, P. J., Spencer, R. G. M., Treat, C. C., Striegl, R. G., et al. (2015). Biodegradability of dissolved organic carbon in permafrost soils and waterways: A meta-analysis. *Biogeosciences Discussions*, *12*(11), 8353–8393. https://doi.org/10.5194/bgd-12-8353-2015

Ward, C. P., & Cory, R. M. (2015). Chemical composition of dissolved organic matter draining permafrost soils. *Geochimica et Cosmochimica Acta*, *167*, 63–79. https://doi.org/10.1016/j.gca.2015.07.001

Weishaar, J. L., Aiken, G. R., Bergamaschi, B. A., Fram, M. S., Fujii, R., & Mopper, K. (2003). Evaluation of specific ultraviolet absorbance as an indicator of the chemical composition and reactivity of dissolved organic carbon. *Environmental Science & Technology*, *37*(20), 4702–4708. https://doi.org/10.1021/es030360x

Wickham, H., Averick, M., Bryan, J., Chang, W., McGowan, L., François, R., et al. (2019). Welcome to the tidyverse. *Journal of Open Source Software*, *4*(43), 1686. https://doi.org/10.21105/joss.01686

Wickland, K. P., Aiken, G. R., Butler, K., Dornblaser, M. M., Spencer, R. G. M., & Striegl, R. G. (2012). Biodegradability of dissolved organic carbon in the Yukon River and its tributaries: Seasonality and importance of inorganic nitrogen. *Global Biogeochemical Cycles*, *26*(4). https://doi.org/10.1029/2012GB004342

Wickland, K. P., Neff, J. C., & Aiken, G. R. (2007). Dissolved organic carbon in Alaskan boreal forest: Sources, chemical characteristics, and biodegradability. *Ecosystems*, *10*(8), 1323–1340. https://doi.org/10.1007/s10021-007-9101-4

Wologo, E., Shakil, S., Zolkos, S., Textor, S., Ewing, S., Klassen, J., et al. (2021). Stream dissolved organic matter in permafrost regions shows surprising compositional similarities but negative priming and nutrient effects. *Global Biogeochemical Cycles*, *35*(1). https://doi.org/10.1029/2020GB006719

Xian, F., Hendrickson, C. L., Blakney, G. T., Beu, S. C., & Marshall, A. G. (2010). Automated broadband phase correction of Fourier transform ion cyclotron resonance mass spectra. *Analytical Chemistry*, *82*(21), 8807–8812. https://doi.org/10.1021/ac101091w

Xu, C., Guo, L., Dou, F., & Ping, C.-L. (2009). Potential DOC production from size-fractionated Arctic tundra soils. *Cold Regions Science and Technology*, *55*(1), 141–150. https://doi.org/10.1016/j.coldregions.2008.08.001